Paper

TRANSCRIPTOME ALTERATIONS IN X-IRRADIATED HUMAN GINGIVA FIBROBLASTS

Robert Weissmann,* Tim Kacprowski,† Michel Peper,‡ Jennifer Esche,* Lars R. Jensen,* Laura van Diepen,* Matthias Port,‡ Andreas W. Kuss,* and Harry Scherthan‡

Abstract—**Ionizing radiation is known to induce genomic lesions, such as DNA double strand breaks, whose repair can lead to mutations that can modulate cellular and organismal fate. Soon after radiation exposure, cells induce transcriptional changes and alterations of cell cycle programs to respond to the received DNA damage. Radiation-induced mutations occur through misrepair in a stochastic manner and increase the risk of developing cancers years after the incident, especially after high dose radiation exposures. Here, the authors analyzed the transcriptomic response of primary human gingival fibroblasts exposed to increasing doses of acute high dose-rate x rays. In the dataset obtained after 0.5 and 5 Gy x-ray exposures and two different repair intervals (0.5 h and 16 h), the authors discovered several radiation-induced fusion transcripts in conjunction with dose-dependent gene expression changes involving a total of 3,383 genes. Principal component analysis of repeated experiments revealed that the duration of the post-exposure repair intervals had a stronger impact than irradiation dose. Subsequent overrepresentation analyses showed a number of KEGG gene sets and WikiPathways, including pathways known to relate to radioresistance in fibroblasts (Wnt, integrin signaling). Moreover, a significant radiation-induced modulation of microRNA targets was detected. The data sets on IR-induced transcriptomic alterations in primary gingival fibroblasts will facilitate genomic comparisons in various genotoxic exposure scenarios.**

*Department of Human Genetics, University Medicine Greifswald and Interfaculty Institute of Genetics and Functional Genomics, University of Greifswald, Greifswald, Germany; †Interfaculty Institute for Genetics and Functional Genomics, Department of Functional Genomics, University Medicine Greifswald, Germany; ‡Institut für Radiobiologie der Bundeswehr in Verbindung mit der Universität Ulm, München, Germany.

The authors declare no conflicts of interest.

For correspondence contact: Andreas W. Kuss, Department of Human Genetics, University Medicine Greifswald and Interfaculty Institute of Genetics and Functional Genomics, University of Greifswald, Greifswald, Germany, or email at **kussa@uni-greifswald.de** or Harry Scherthan, email at **scherth@web.de**.

Supplemental Digital Content is available in the HTML and PDF versions of this article on the journals Web site www.health-physics.com.

(*Manuscript accepted 22 September* 2015)

0017-9078/16/0

DOI: 10.1097/HP.0000000000000419

Health Phys. 111(2):75–84; 2016

Key words: genetic effects; radiation; radiation effects; repair; cellular; x rays

INTRODUCTION

THE LAST decades have seen a growing application of ionizing radiation (IR) in medical diagnostics and radiology. While these applications usually involve very low doses of IR, acute high dose rate exposures are known from a number of radiation accidents. These often involve exposition to one single acute dose of IR that induces acute radiation sickness (ARS) and localized injuries and may lead to stochastic consequences. While deterministic damages relate to IR-induced cell death and necrosis, lower doses induce stochastic effects like mutations that may alter a cell's fate and contribute to cancerogenesis. Altered gene expression patterns are seen as an important indicator for the cellular response to such IR-induced genetic defects, and it is widely believed that the study of transcriptomic consequences can provide important insights into the processes involved (e.g., Paul and Amundson et al. 2003). Moreover, there have been several successful attempts in the use of gene expression signatures for the prediction/reconstruction of radiation dose using nucleated cells of the peripheral blood (e.g., Amundson 2008; Brengues et al. 2010; Paul and Amundson 2011; Paul et al. 2011; Port et al. 2012).

Besides internal organ systems, the skin plays an important role in diagnostics and management of radiation accident victims or in cancer therapy, when IR-exposure compromises its barrier function and leads to resulting inflammatory reactions (Dorr and Meineke 2011). Since fibroblasts are important for tissue repair, primary human gingival fibroblasts (HGF) were chosen as a cellular model for the study presented here. Fibroblasts play a central role in the maintenance of the structural integrity of connective tissues, as they continuously secrete precursors of all the components of the extracellular matrix (ECM), the composition

of which determines the physical properties of connective tissues (e.g., Watt and Fujiwara 2011).

Most previous studies have applied microarray-driven gene expression analysis to gain insights concerning the genomic consequences of radiation exposure. In this investigation, an RNA-sequencing approach was used to investigate the impact of different acute doses of x-irradiation on human gingival fibroblasts, also taking into account different post-exposure (repair) intervals; i.e., the time span between irradiation and harvesting of the cells. The obtained results show dose-dependent changes in gene expression after two different repair intervals for a total of 3,383 genes. Principal component analysis (PCA) of the obtained data sets showed that the duration of the repair interval had a more pronounced impact than the irradiation doses applied. Moreover, over-representation studies revealed a number of KEGG gene sets and WikiPathways to be overrepresented among the genes differentially expressed over the different repair intervals and showed modulation of microRNA targets as a consequence of irradiation treatment.

MATERIALS AND METHODS

Cell culture and radiation treatment

Human gingival fibroblasts (HGFs) were obtained from Provitro AG (Berlin, Germany). The HGFs (passage 9) were cultured at 37 °C using Fibroblast Growth Medium (Provitro, Berlin, Germany) without antibiotics. Cells were grown to near confluency and irradiated in 175 cm^2 bottles. Thereafter, cells were returned to the incubator or detached from the flasks by a brief treatment with trypsin/EDTA (PAA Laboratories, Dartmouth, MA, USA). After resuspension in a small volume of medium in a cell culture tube, these were snap-frozen in liquid N_2 and stored at −86 °C until RNA preparation. With the exception of one combination of radiation dose and repair interval (0.5 Gy and 16 h), which was not used for quantitative analyses, experiments were performed in duplicates or triplicates (see Table Supplemental Digital Content 1, http://links.lww.com/HP/A52 which contains general information on the datasets).

Irradiation

Cells were irradiated at room temperature with 240 kV x rays at 13 mA (YXLON Maxishot; Hamburg, Germany) filtered with 3 mm beryllium at a dose rate of 1 Gy min^{-1}. Absorbed dose was measured with a PTW Unidos dosimeter (PTW Freiburg GmbH, Freiburg, Germany). Control cells were sham-irradiated.

RNA sequencing

RNA sequencing was performed on a SOLiD 5500xl Genetic Analyzer (Life Technologies, Carlsbad, NM, USA). RNA from experimentally treated HGFs was extracted as follows. The cells were homogenized using a Polytron (VWR) device and then treated with TRIzol (Life Technologies, Carlsbad, NM, USA). Next, the rRNA was removed from the RNA samples by use of a RiboZero Kit (Epicentre, Madison, WI, USA) according to the manufacturers' instructions. The thus purified RNA was fragmented by chemical hydrolysis, phosphorylated and purified. Adaptors were ligated to the RNA fragments, which subsequently were reverse-transcribed into cDNA. This was then used for preparation of a sequencing library according to the protocols provided by the manufacturer of the sequencer (see also Bouter et al. 2014) and sequenced using the settings and recommended chemicals for sequencing 75 nucleotides in the forward direction and 35 nucleotides in the reverse direction (Life Technologies, Carlsbad, NM).

Sequence reads were mapped to the human genome reference sequence hg19 (ftp://hgdownload.cse.ucsc.edu/goldenPath/hg19/) using the workflow 'whole.transcriptome.pe' of LifeScope-v2.5.1-r0 (Life Technologies, Carlsbad, NM, USA). Reads that mapped to RefSeq coding exons (http://hgdownload.cse.ucsc.edu/goldenPath/hg19/database/refGene.txt.gz) and matching the coding strand were considered coding RNAs. All other mapping reads were considered non-coding.

RNA-sequencing yielded between 23 and 64 millions of reads per sample (see also Table Supplemental Digital Content 1, http://links.lww.com/HP/A52).

Differential expression analysis

Quality control and principal component analysis (PCA) were conducted with variance-stabilized read count data. The PCA was implemented in R, relying on the *prcomp* function. Each of the 18 principal components was interpreted as outcome for multiple linear regression models incorporating the sample parameters to be analyzed as exposures.

Differential expression analysis was performed using the R package DESeq2 (Love et al. 2014). Due to the applied mathematical models, DESeq2 relies on raw count data. Hence, in contrast to the quality control and PCA mentioned above, which were performed on normalized data, the authors did not perform normalization of the data prior to differential expression analysis. DESeq2 employs empirical Bayes shrinkage to estimate model parameters and fits negative binomial generalized linear models per gene. In contrast to maximum likelihood estimation, the Bayes shrinkage can automatically account for gene-specific variation in the count data and is more generalizable. The significance of differential expression was assessed by Benjamini-Hochberg corrected p-values of a Wald test of the model coefficients corresponding to the sample parameters. The threshold for significance was set to $p = 0.05$. In R notation, the final model for differential expression was *count ~ dT + Gray + seqStart + PC1 + PC2 + PC3*. *Count*

is the read counts for a gene, *dT* is the repair interval (time span between irradiation and cell harvest), *Gray* is the radiation dose in Gy, *seqStart* denotes the individual experiments, and *PCi* is the ith principal component from the aforementioned PCA. The model was restricted to the first three PCs. These explain already more than 50% of the variance in the data. No more PCs were included since the increase in explained variance per PC as well as the PC Eigenvalues drop sharply for PC4–PC18. This avoids over-specification of the model and allows for easier interpretation.

Annotation analysis

An overrepresentation analysis (ORA) was conducted to learn about the biological function and to understand the putative role of differentially expressed genes in specific biological pathways. The ORA was done as implemented in GO-Elite (Zambon et al. 2012), relying on the default parameters and the EnsMart62Plus annotation for humans. The EnsMart62Plus comprises annotation from KEGG (Kanehisa and Goto 2000), WikiPathways (Kelder et al. 2012), transcription factor-target relationships from the Amadeus Metazoan compendium (Linhart et al. 2008) and the PAZAR transcription factor and regulatory sequence database (Portales-Casamar et al. 2007), and microRNA target sets as compiled in AltAnalyze (Emig et al. 2010). The complete list of all detected genes served as background for the ORA. Gene symbols were automatically mapped to Ensembl IDs by GO-Elite. As foreground (or gene set of interest), the parameter specific list of significantly differentially expressed genes was used. That is, the authors performed ORA for each parameter (dT, gray, seqStart, PC1, PC2, PC3) of the model used to assess differential expression.

RESULTS

Radiation-induced fusion transcripts

RNA sequencing revealed a few radiation-induced fusion transcripts in comparison to untreated cells (Table 1). Only one of these, involving the first exon each of RMRP (RNA component of mitochondrial RNA processing endoribonuclease; OMIM: 157660) and RPPH1 (ribonuclease P RNA component H1; OMIM: 608513), includes exons from two different chromosomes (Chr 9 and Chr 14, respectively). This fusion transcript was found in two independent samples that were exposed to 0.5 Gy and were harvested after different repair intervals. The remaining fusion transcripts were all intrachromosomal and contained exons from relatively closely spaced neighboring genes (Table 1). A clear association of the frequency of occurrence with irradiation dose and/or duration of the repair interval was not evident.

Radiation-induced effects on gene expression in HGFs

Next, the numbers of genes with dose-dependent expression modulation 0.5 h and 16 h after irradiation were investigated as shown in the Venn diagram in Fig. 1. A subset of these genes shows overlapping expression effects at different time points after irradiation; e.g., 218 genes show a dose-dependent increase in expression 0.5 h and 16 h after IR (see Tables Supplemental Digital Content 2–5, (http://links.lww.com/HP/A53, http://links.lww.com/HP/A54, http://links.lww.com/HP/A55, http://links.lww.com/HP/A56) which show differentially regulated genes in a dose dependent manner after different repair intervals).

For four genes, reverse regulation depending on the repair interval was observed. The zinc finger gene *ZMYND12* (Zinc Finger, MYND-Type Containing 12) and *TSSK1B* (Testis-Specific Serine Kinase 1B) showed a downregulation with increasing dose 0.5 h after exposure and dose-dependent upregulation after 16 h (Fig. 1b and c). The *LYG1* (Lysozyme G-Like 1) gene and the Nucleolar Complex Associated 2 Homolog (*S. cerevisiae*) pseudogene (*LOC401010)*, on the other hand, displayed dose-dependent upregulation at 0.5 h and down-regulation at 16 h post IR (Fig. 1a and b).

Principal component analysis (PCA)

PCA of the RNA-Seq data (Table Supplemental Digital Content 6, http://links.lww.com/HP/A64 which contains the complete list of differentially expressed genes) revealed that gene expression was comparatively homogenous within the samples from a given experiment; i.e., the first three principal components (PCs) were strongly associated with individual experiments (as determined by multiple linear regression) (Fig. 2, 3b). Differential expression based on radiation dose and and/or duration of the repair interval had only a subordinate influence on clustering of the samples, as only the third, fifth, and tenth PC were associated with either the repair interval or the IR dose (Fig. 2).

Annotation analysis

In order to understand the biological function and the putative role of differentially expressed genes in specific biological pathways, an overrepresentation analysis (ORA) was performed. With respect to radiation dose, only one significant overrepresentation was detected; i.e., targets of the transcription factor p53 (Table 2). This was mainly due to the upregulation of pro-apoptotic BBC3 (BCL2 Binding Component 3) and DDB2 (Damage-Specific DNA Binding Protein 2) with an average log2-fold change (L2FC) of 0.046.

When looking at post-irradiation repair intervals, on the other hand, a slightly larger number of KEGG gene sets and WikiPathways were overrepresented among the differentially expressed protein coding genes. In general, these gene sets were downregulated on average, and only a few gene sets showed a slight average upregulation (Table 2).

It is interesting that genes targeted by microRNAs showed a reverse behavior: 395 microRNA target sets showed an average upregulation, while only two exhibited

Table 1. Radiation-induced fusion transcripts in comparison to untreated cells.[a]

Irradiation and duration of post experimental incubation	Sample #	Exon 1	E1-reference	E1-strand	E1-start	E1-end	Exon 2	E2-reference	E2-strand	E2-start	E2-end	E1-size	E2-size	E1-read-count	E2-read-count	E1-RPKM	E2-RPKM	Exon-distance	Total-pair-end	Unique-pair-end	Total-single-read	Unique-single-read	JCV
0.5Gy, 16h	280	***ARPC4-8***	chr3	+	9845527	9845697	***TTLL3-3***	chr3	+	9852305	9852393	171	89	229	34	77,41	22,08	6608	2	2	5	4	87,37
2Gy, 16h	281	***ARPC4-8***	chr3	+	9845527	9845697	***TTLL3-3***	chr3	+	9852305	9852393	171	89	243	21	81,79	13,58	6608	2	2	2	2	73,2
0.2Gy, 0.5h	273	***CTBS-6***	chr1	−	85028940	85029101	***GNG5-3***	chr1	−	84967509	84967653	162	145	99	61	23,78	16,37	61287	5	2	7	2	47,36
0.5Gy, 6h	189	***CTBS-6***	chr1	−	85028940	85029101	***GNG5-3***	chr1	−	84967509	84967653	162	145	108	44	25,94	11,81	61287	2	2	3	3	62,4
5Gy, 6h	191	***CTBS-6***	chr1	−	85028940	85029101	***GNG5-3***	chr1	−	84967509	84967653	162	145	134	97	19,69	15,93	61287	9	3	5	2	84,03
0.5Gy, 0.5h	188	***RMRP-1***	chr9	−	35657748	35658015	***RPPH1-1***	chr14	−	20811230	20811570	268	341	173075	268587	25044,46	30545,18	N/A	80	47	2	2	100
0.5Gy, 6h	189	***RMRP-1***	chr9	−	35657748	35658015	***RPPH1-1***	chr14	−	20811230	20811570	268	341	169633	275209	24625,37	31398,98	N/A	131	72	3	2	100

[a]E1/2-strand: ± strand.

E1/2-start: start position (hg19)

E1/2-end: end position (hg19)

E1/2-size: exon size in bp.

E1/2-readcount: number of reads that map on the first/second exon.

E1/2-RPKM: reads Per kbp Per Million Reads (RPKM) exon-1 from F3.

Exon-distance: distance between two exons (not applicable if exons are on different chromosomes).

Total-PR-evidence: total paired-end evidence for the junction.

Unique-PR-evidence: unique paired-end evidence for the junction.

Total-SR-evidence: total single-read evidence for the junction.

Unique-SR-evidence: unique single-read evidence for this junction.

JCV: junction confidence value.

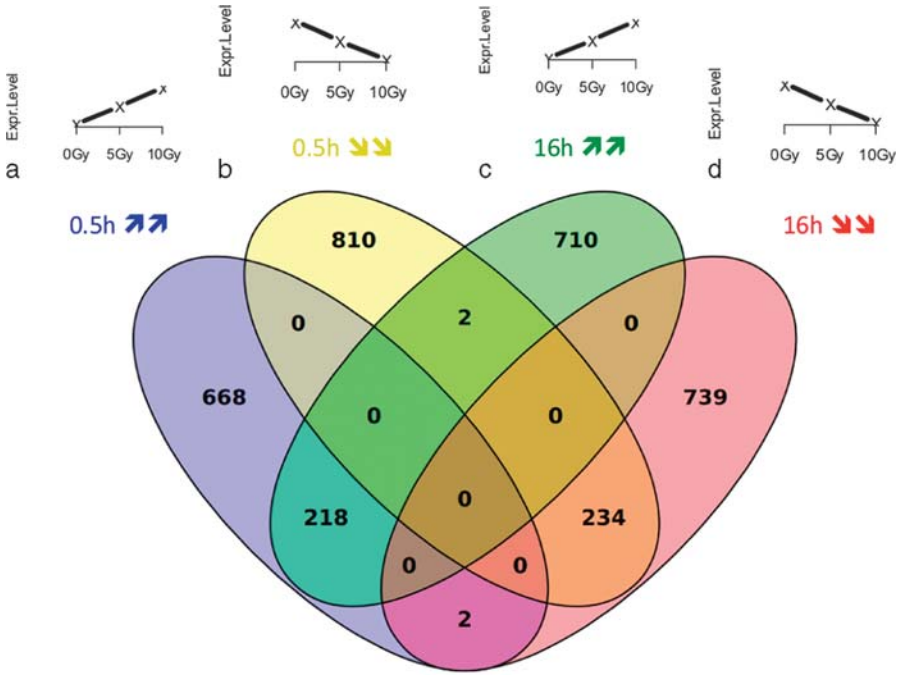

Fig. 1. Venn diagram [developed using Venny (Oliveros 2015)] showing the numbers of genes with dose-dependent expression increase 0.5 h (a) and 16 h (c) after IR, the numbers of genes with dose-dependent expression decrease 0.5 h (b) and 16 h (d) after IR. An explicit list of the genes with altered expression is given in Tables Supplemental Digital Content 2–5, http://links.lww.com/HP/A54, http://links.lww.com/HP/A55, http://links.lww.com/HP/A56.

average downregulation (Table Supplemental Digital Content 7 http://links.lww.com/HP/A57). Notably, though, for many overrepresented gene sets, especially for the target sets of microRNAs, the standard deviation of the log2-fold change (L2FC) was larger than the absolute average L2FC, which may indicate general modulation of microRNA targets through a widespread effect on microRNA expression.

Since there was no evident order relationship of individual experiments (the magnitude of effects in experiment A or B cannot be distinguished), the analysis could only focus on dysregulation, which means that gene sets could only be evaluated irrespective of the direction of fold changes. This revealed similar gene sets to be overrepresented as observed for the repair intervals (Table Supplemental Digital Content 7, http://links.lww.com/HP/A57); e.g., Parkinson's, Alzheimer's, and Huntington's disease (KEGG-hsa05012, KEGG-hsa05010, KEGG-hsa05016, respectively), Oxidative phosphorylation (KEGG-hsa00190), Citrate cycle (KEGG-hsa00020), Ribosome (KEGG-hsa03010) and Proteasome (KEGG-hsa03050). Also 23 target sets of microRNAs were found to be overrepresented (Table Supplemental Digital Content 7 http://links.lww.com/HP/A57).

In addition to that, a search for genes that were differentially expressed across the first three PCs of the count data (Table Supplemental Digital Content 7, http://links.lww.com/HP/A57) was performed. As these PCs were associated with individual experiments, again the direction of fold-changes could not be considered, and only dysregulation (instead of PC-specific up- and downregulation) was taken into account.

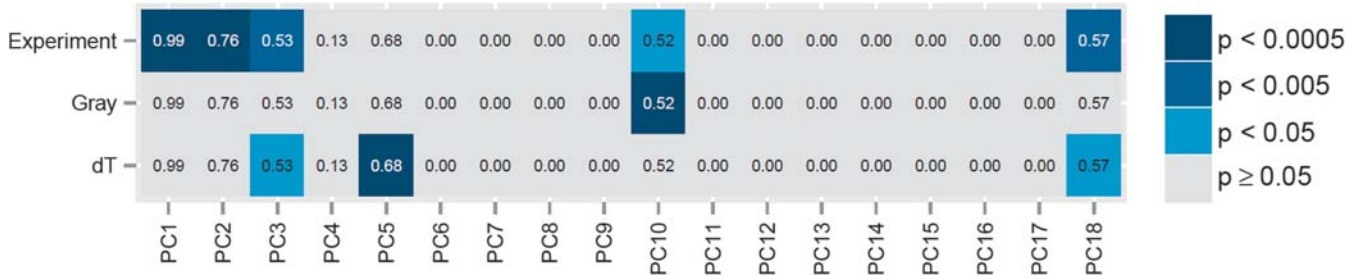

Fig. 2. Association of principal components to sample properties. dT - repair interval; Gray - radiation dose in Gy; Experiment - individual experiments; PCi - ith principal component. Blue shading indicates significant association between a PC and a sample parameter. Numbers in cells represent the adjusted R-squared value for the linear regression models.

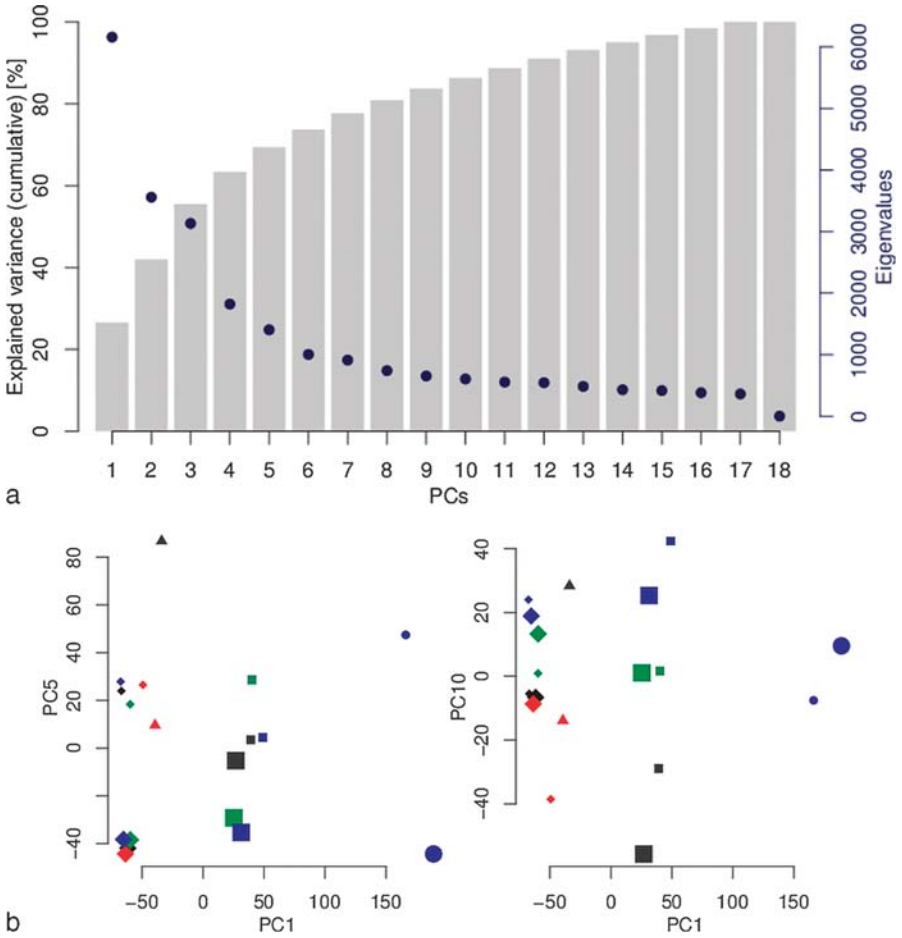

Fig. 3. Principal component analysis results. (a) Importance of principal components (PC). The grey bars depict the cumulative explained variance in the data when considering PC1 to PCi; e.g., the third bar, corresponding to PC3, shows the variance in the data explainable by PC1, PC2, and PC3 together. The blue dots indicate the Eigenvalues of the respective PCs. The Eigenvalues are a measure for how far the data spread along the given PC. This information is closely related to the explained variance per PC (the more variance is explained by the PC, the further the data are spread along it). (b) Scatter plots of the samples projected onto PC1 vs. PC5 (left) and PC1 vs. PC10 (right). The shape of the symbol corresponds to the individual experiments. The time between irradiation and sequencing is indicated by the size of the symbols (larger symbol, longer time). The color shows the radiation dose (black: 0 gray, red: 0.5 gray, green: 5 gray, blue: 10 gray). The sorting of symbols along the x-axis visualizes the strong association of PC1 to the individual experiments. Similarly, PC5 sorts the symbols according to their size, indicating its association to the time between irradiation and sequencing. PC10's association to the radiation dosage becomes evident by the sorting of the symbols according to their colors.

Among the genes differentially expressed across the first PC, several overrepresented GPCR related gene sets were observed (WP24, WP455, WP501, WP334, WP117, WP58). Overrepresentation of targets of specific microRNAs, however, was absent. Nevertheless, several microRNA-related gene sets such as microRNAs involved in DNA damage response (WP1545), microRNA-targeted genes in adipocytes (WP2001), and microRNA targets in ECM and membrane receptors (WP2911) were overrepresented (Table Supplemental Digital Content 7, http://links.lww.com/HP/A57).

Across the second PC, differentially expressed genes were overrepresented in disease-related pathways, protein synthesis, and degradation related gene sets. Here, 24 over-represented microRNA target sets were counted (Table Supplemental Digital Content 7, http://links.lww.com/HP/A57).

When focusing on the genes differentially expressed across the third PC, which was also associated with the duration of the repair interval, signaling-related gene sets like the TGF-beta (Receptor) signaling pathway (KEGG-hsa04350, WP366), the Wnt signaling pathway (KEGG-hsa04310), and the (m)TOR signaling (pathway) (KEGG-hsa04150, WP1471) were found to be overrepresented. In addition to that, several cancer-related gene sets, such as Prostate cancer, Colorectal cancer, and Acute myeloid leukemia (KEGG-hsa05215, KEGG-hsa05210, KEGG-hsa05221, respectively), were over-represented as well as microRNA-related gene sets such as microRNA-targeted genes in lymphocytes, muscle cells, epithelium, and squamous cells (WP2004, WP2005, WP2002, WP2006, respectively). With respect to microRNA target gene sets, a total of 234 showed overrepresentation

Table 2. Targets of the transcription factor p53.

Parameter	Annotation class	Term	BH-adjusted permutation p-value	# genes differentially regulated	# genes in Dataset	# genes annotated	Direction of avg regulation
Radiation dose	TFTargets	p53(Source:Kannan-Amadeus)	0.0180	2	32	32	up
Repair interval	KEGG	Ribosome (hsa03010)	0.0072	77	88	95	down
Repair interval	KEGG	Huntington's disease (hsa05016)	0.0072	84	174	182	down
Repair interval	KEGG	Oxidative phosphorylation (hsa00190)	0.0072	62	118	139	down
Repair interval	KEGG	Parkinson's disease (hsa05012)	0.0072	59	116	130	down
Repair interval	KEGG	Alzheimer's disease (hsa05010)	0.0072	71	158	173	down
Repair interval	KEGG	Spliceosome (hsa03040)	0.0072	49	124	153	down
Repair interval	KEGG	Ubiquitin mediated proteolysis (hsa04120)	0.0072	47	135	135	down
Repair interval	KEGG	Proteasome (hsa03050)	0.0072	20	44	57	down
Repair interval	KEGG	Lysine degradation (hsa00310)	0.0072	21	48	52	up
Repair interval	KEGG	Protein processing in endoplasmic reticulum (hsa04141)	0.0072	54	165	183	down
Repair interval	KEGG	Protein export (hsa03060)	0.0072	12	23	23	down
Repair interval	KEGG	Shigellosis (hsa05131)	0.0072	23	61	61	up
Repair interval	KEGG	Bacterial invasion of epithelial cells (hsa05100)	0.0128	26	70	70	down
Repair interval	KEGG	Endocrine and other factor-regulated calcium reabsorption (hsa04961)	0.0182	19	49	49	up
Repair interval	KEGG	RNA transport (hsa03013)	0.0470	49	147	161	down
Repair interval	KEGG	Insulin signaling pathway (hsa04910)	0.0479	44	136	143	up
Repair interval	KEGG	Circadian rhythm - mammal (hsa04710)	0.0479	9	22	22	up
Repair interval	WikiPathways	Cytoplasmic Ribosomal Proteins (WP477)	0.0135	73	87	90	down
Repair interval	WikiPathways	Electron Transport Chain (WP111)	0.0135	50	90	105	down
Repair interval	WikiPathways	Oxidative phosphorylation (WP623)	0.0135	30	52	62	down
Repair interval	WikiPathways	Alpha6-Beta4 Integrin Signaling Pathway (WP244)	0.0135	35	67	68	up
Repair interval	WikiPathways	Translation Factors (WP107)	0.0135	26	50	50	down
Repair interval	WikiPathways	miR-targeted genes in squamous cell - TarBase (WP2006)	0.0135	58	149	155	up
Repair interval	WikiPathways	Histone Modifications (WP2369)	0.0135	30	64	66	down
Repair interval	WikiPathways	Androgen receptor signaling pathway (WP138)	0.0135	36	87	89	up
Repair interval	WikiPathways	Proteasome Degradation (WP183)	0.0135	26	58	60	down
Repair interval	WikiPathways	Apoptosis-related network due to altered Notch3 in ovarian cancer (WP2864)	0.0135	23	52	52	down

(Table Supplemental Digital Content 7, http://links.lww.com/HP/A57).

DISCUSSION

When cells are exposed to IR, their response often depends on the dose and the dose rate. For lesions leading to stochastic damages and ultimately cancer, the DNA is the relevant molecule. A first line response to IR is the adjustment of the transcriptional activity to the needs of a damaged cell that seeks to undergo repair. In agreement, many labs have reported transcriptome responses associated with radiation exposure, some of which are dose dependent (e.g., Amundson et al. 2000; Ghandhi et al. 2008, 2010, 2015).

Until recently, the standard technique to quantify large numbers of mRNA transcripts simultaneously for such studies was the analysis of microarrays that could analyze up to 30,000 different mRNAs (Amundson 2008). Still, as these assays depend on the hybridization of preselected gene-specific probes, there are several disadvantages, such as the limitation to known sequences, a comparatively poor range of quantification, low sensitivity, and specificity (Marioni et al. 2008). Moreover, unspecific binding hampers the detection of lowly expressed transcripts and the quantification of differentially expressed genes with fold-changes below two (Wang et al. 2009). Here, a next generation sequencing approach (RNA-Seq) was used, which allowed circumvention of many of the described disadvantages (Wang et al. 2009). In particular, RNA-Seq does not rely on preselected known transcripts and thus allows not only the detection of novel protein-coding as well as non-coding transcripts but also the discovery of fusion transcripts.

Here, the authors observed for the first time radiation-induced fusion transcripts in irradiated HGFs whose number, however, was very limited. This could, in part, be due to the short length of the individual sequence reads produced by their sequencing platform. Still, it is more likely that there are indeed only very few fusion transcripts induced by the IR conditions applied. One possibility is that fusion transcripts of genes from different chromosomes

arise from reciprocal translocations that have been detected by molecular cytogenetics at a low rate in low-LET x-irradiated cells (Whitehouse et al. 2005; BEIR VII 2006). Fusion transcripts from cis are likely the result of intrachromosomal deletions/fusions, which by molecular cytogenetic methods go largely undetected. A prevalence of fusion transcripts from deletions in this investigation goes along with the notion that high dose/dose rate exposures lead predominantly to genomic losses (Finn et al. 2004; Muradyan et al. 2011). Moreover, the protein coding part, which is the subject of this investigation, comprises only about 2% of the human genome. Since low-LET irradiation seeds about 25 DSB Gy^{-1} $cell^{-1}$ in the fibroblast genome (Stenerlow et al. 2003; Antonelli et al. 2015; own unpublished observations), the bulk of IR-induced stochastic events will most likely affect extragenic regions and thus remain undetected by transcriptomic analyses. In all, it will be of interest to compare the number of induced (detected) fusion transcripts with that of cytogenetically visible translocations. As an alternative to fusion-transcript formation by translocations/deletions, it can be envisaged that alternative trans-splicing (for review see Horiuchi and Aigaki 2006) may be a source of fusion transcripts, especially since clonal expansion of a particular aberration-carrying cell is not required. Future investigation in this direction will have to elucidate this route further.

Comparing these results with previous findings from the literature reveals only very few datasets that can be taken into account, as most studies focused on different tissues or cell types. Moreover, many of these investigations primarily dealt with findings from cohorts comprising individuals that were subject to different radiation exposure scenarios rather than controlled cell cultures in a standardized setting as used in the present study. Interestingly, the IR-induced gene expression signature of white blood cells (Paul and Amundson 2008) comprised, among others, *CDKN1A, FDXR, SESN1, BBC3 and PHPT1*, of which *BBC3* (BCL2 binding component 3) was also showing a dose-dependent increase in this fibroblast study (0.5-h repair time).

The differences between studies likely relate to cell type-specific effects. A study focusing on fibroblasts presented about 60 differentially expressed genes upon IR exposure (Ghandhi et al. 2010), several of which also showed expression differences in this study (see also Tables Supplemental Digital Content 8-10 (http://links.lww.com/HP/A58, http://links.lww.com/HP/A59, http://links.lww.com/HP/A60) that show differential expression results for the genes described by Ghandhi et al. 2010). Concerning the quality and quantity of expression changes, the effects noted by Ghandhi et al. (2008), however, were often at variance to the observations made here, which is most likely due to experimental setup, differences in radiation quality, and dose rates applied in the two studies: Ghandhi et al. used high LET alpha irradiation with ^{4}He ions at a dose rate of 0.5 Gy min^{-1}, while this study applied low LET 240 kV x rays at 1 Gy min^{-1}. In line with this reasoning, different DSB yields and qualities have been observed for different radiation qualities (Prise et al. 1998; Antonelli et al. 2015).

As to the results from overrepresentation analysis, the authors found a number of overrepresented cancer-related gene sets, such as prostate cancer, colorectal cancer, and acute myeloid leukemia across the third principal component (i.e., repair interval), as well as several cancer-related signaling gene sets, one example being the TGF-beta receptor signaling pathway, which plays a role in cancer (for review see Drabsch and ten Dijke 2012) but also in the response to ionizing radiation exposure of the skin (see Schultze-Mosgau et al. 2006). In this respect, it is of note that the radiation-induced dysregulation of skin fibroblasts studied here is involved in fibrosis (Bentzen 2006; Avraham et al. 2010) where TGF-beta is known to play an important etiological role (e.g., Forrester et al. 2013).

Interestingly, in a previous study investigating follistatin in a set of primary fibroblast cells derived from patients who developed fibrosis after radiotherapy, the authors observed reduced follistatin (*FST*) gene expression levels as compared to controls at both basal levels and after IR (Forrester et al. 2013), which compares to this study where *FST* was among the genes that showed consistent dose-dependent downregulation 16 h after IR (Table Supplemental Digital Content 6 http://links.lww.com/HP/A64).

Further overrepresented gene sets were the mTor pathway (reviewed by Zhou and Huang 2010) and the Wnt signaling pathway. Wnt signaling plays an important role in the control of cell morphology, motility, and proliferation and maintains the homeostasis of tissues including the skin, where abnormal regulation of this pathway leads to neoplastic proliferation (Li et al. 2015) and beta-Catenin, a key component in the Wnt-signaling pathway, directs the radiation response of skin fibroblasts (Gurung et al. 2009).

Interestingly, also the integrin-signaling pathway was among the gene sets detected by the ORA to be differentially expressed over different repair intervals. This is of note since integrin signaling has been observed to be modulated by IR and relates to radioresistance. For example, it was found that β1-integrin signaling confers radioresistance to breast cancer cells (Ahmed et al. 2013).

In addition, the results presented here repeatedly showed the overrepresentation of microRNA-genes. Interestingly, deregulation of microRNA gene expression was noted in leukocytes of chronically radiation-exposed humans (Abend et al. 2015).

However, for many overrepresented gene sets, especially for the target sets of microRNAs, the standard deviation of the L2FC was larger than the absolute average L2FC, which makes it difficult to establish consistent up- or down-regulation and

rather points to some general dysregulation of microRNA target sets. Further experiments are required to elucidate this point in more detail.

CONCLUSION

This RNAseq NGS study on the consequences of IR exposure of human primary fibroblasts disclosed novel IR-induced fusion transcripts, which underline the translocation and deletion-inducing potential of IR exposure at the transcriptional level. Furthermore, principal component analysis followed by overrepresentation analyses revealed a number of overrepresented KEGG gene sets and WikiPathways among the genes differentially expressed during the two repair intervals studied and a significant radiation-induced modulation of microRNA targets. The authors observed the IR modulation of pathways known to relate to radioresistance in fibroblasts (Wnt, integrin signaling), validating the experimental approach. The observed alterations in other pathways will be the subject of further analysis. Finally, the generated NGS transcriptomic data sets on the genotoxic IR exposure of gingival primary fibroblasts will facilitate genomic comparisons in various genotoxic exposure scenarios.

Acknowledgments—We thank Christian Sperling and Corinna Jensen for excellent technical help. AWK received funding for this project through the German Federal Ministry of Defense (E/U2AD/CF520/DF554) and the European Union (EFRE). TK's position is funded by the BMBF/"Unternehmen Region" as part of the ZIK-FunGene.

REFERENCES

Abend M, Azizova T, Muller K, Dorr H, Doucha-Senf S, Kreppel H, Rusinova G, Glazkova I, Vyazovskaya N, Unger K, Braselmann H, Meineke V. Association of radiation-induced genes with noncancer chronic diseases in Mayak workers occupationally exposed to prolonged radiation. Radiat Res 183: 249–261; 2015.

Ahmed KM, Zhang H, Park CC. Nf-kappab regulates radioresistance mediated by beta1-integrin in three-dimensional culture of breast cancer cells. Cancer Res 73:3737–3748; 2013.

Amundson SA. Functional genomics and a new era in radiation biology and oncology. Bioscience 58:491–500; 2008.

Amundson SA, Bittner M, Fornace AJ, Jr. Functional genomics as a window on radiation stress signaling. Oncogene 22: 5828–5833; 2003.

Amundson SA, Do KT, Shahab S, Bittner M, Meltzer P, Trent J, Fornace AJ, Jr. Identification of potential mRNA biomarkers in peripheral blood lymphocytes for human exposure to ionizing radiation. Radiat Res 154:342–346; 2000.

Antonelli F, Campa A, Esposito G, Giardullo P, Belli M, Dini V, Meschini S, Simone G, Sorrentino E, Gerardi S, Cirrone GA, Tabocchini MA. Induction and repair of DNA dsb as revealed by h2ax phosphorylation foci in human fibroblasts exposed to low- and high-let radiation: relationship with early and delayed reproductive cell death. Radiat Res 183:417–431; 2015.

Avraham T, Yan A, Zampell JC, Daluvoy SV, Haimovitz-Friedman A, Cordeiro AP, Mehrara BJ. Radiation therapy causes loss of dermal lymphatic vessels and interferes with lymphatic function by tgf-beta1-mediated tissue fibrosis. Am J Physiol Cell Physiol 299:C589–605; 2010.

BEIR VII. Health risks from exposure to low levels of ionizing radiation. BEIR VII—phase 2. Washington, D.C.: National Academy Press; 2006.

Bentzen SM. Preventing or reducing late side effects of radiation therapy: radiobiology meets molecular pathology. Nat Rev Cancer 6:702–713; 2006.

Bouter Y, Kacprowski T, Weissmann R, Dietrich K, Borgers H, Brauss A, Sperling C, Wirths O, Albrecht M, Jensen LR, Kuss AW, Bayer TA. Deciphering the molecular profile of plaques, memory decline and neuron loss in two mouse models for Alzheimer's disease by deep sequencing. Front Aging Neurosci 6:75; 2014.

Brengues M, Paap B, Bittner M, Amundson S, Seligmann B, Korn R, Lenigk R, Zenhausern F. Biodosimetry on small blood volume using gene expression assay. Health Phys 98:179–185; 2010.

Dorr H, Meineke V. Acute radiation syndrome caused by accidental radiation exposure—therapeutic principles. BMC Med 9: 126; 2011.

Drabsch Y, ten Dijke P. TGF-beta signalling and its role in cancer progression and metastasis. Cancer Metastasis Rev 31: 553–568; 2012.

Emig D, Salomonis N, Baumbach J, Lengauer T, Conklin BR, Albrecht M. Altanalyze and domaingraph: analyzing and visualizing exon expression data. Nucleic Acids Res 38: W755–762; 2010.

Finn SP, Smyth P, O'Regan E, Cahill S, Flavin R, O'Leary J, Sheils O. Array comparative genomic hybridisation analysis of gamma-irradiated human thyrocytes. Virchows Arch 445: 396–404; 2004.

Forrester HB, Ivashkevich A, McKay MJ, Leong T, de Kretser DM, Sprung CN. Follistatin is induced by ionizing radiation and potentially predictive of radiosensitivity in radiation-induced fibrosis patient derived fibroblasts. PLoS One 8: e77119; 2013.

Ghandhi SA, Ming L, Ivanov VN, Hei TK, Amundson SA. Regulation of early signaling and gene expression in the alpha-particle and bystander response of imr-90 human fibroblasts. BMC Med Genomics 3:31; 2010.

Ghandhi SA, Smilenov LB, Elliston CD, Chowdhury M, Amundson SA. Radiation dose-rate effects on gene expression for human biodosimetry. BMC Med Genomics 8:22; 2015.

Ghandhi SA, Yaghoubian B, Amundson SA. Global gene expression analyses of bystander and alpha particle irradiated normal human lung fibroblasts: synchronous and differential responses. BMC Med Genomics 1:63; 2008.

Gurung A, Uddin F, Hill RP, Ferguson PC, Alman BA. Beta-catenin is a mediator of the response of fibroblasts to irradiation. Am J Pathol 174:248–255; 2009.

Horiuchi T, Aigaki T. Alternative trans-splicing: a novel mode of pre-mRNA processing. Biol Cell [under the auspices of the European Cell Biology Organization] 98:135–140; 2006.

Kanehisa M, Goto S. Kegg: Kyoto encyclopedia of genes and genomes. Nucleic Acids Res 28:27–30; 2000.

Kelder T, van Iersel MP, Hanspers K, Kutmon M, Conklin BR, Evelo CT, Pico AR. Wikipathways: building research communities on biological pathways. Nucleic Acids Res 40:D1301–1307; 2012.

Li J, Ji L, Chen J, Zhang W, Ye Z. Wnt/-catenin signaling pathway in skin carcinogenesis and therapy. Biomed Res Int 964842: 2015; 2015.

Linhart C, Halperin Y, Shamir R. Transcription factor and microrna motif discovery: the Amadeus platform and a compendium of metazoan target sets. Genome Res 18:1180–1189; 2008.

Love MI, Huber W, Anders S. Moderated estimation of fold change and dispersion for RNA-seq data with deseq2. Genome Biol 15:550; 2014.

Marioni JC, Mason CE, Mane SM, Stephens M, Gilad Y. RBA-seq: an assessment of technical reproducibility and comparison with gene expression arrays. Genome Res 18: 1509–1517; 2008.

Muradyan A, Gilbertz K, Stabentheiner S, Klause S, Madle H, Meineke V, Ullmann R, Scherthan H. Acute high-dose x-radiation-induced genomic changes in a549 cells. Radiat Res 175:700–707; 2011.

Oliveros JC. Venny. An interactive tool for comparing lists with Venn's diagrams [online]; 2015. Available at ***http://bioinfogp.cnb.csic.es/tools/venny/index.html***. Accessed 1 August 2015.

Paul S, Amundson SA. Development of gene expression signatures for practical radiation biodosimetry. Int J Radiat Oncol Biol Phys 71:1236–1244; 2008.

Paul S, Amundson SA. Gene expression signatures of radiation exposure in peripheral white blood cells of smokers and nonsmokers. Int J Radiat Biol 87:791–801; 2011.

Paul S, Barker CA, Turner HC, McLane A, Wolden SL, Amundson SA. Prediction of in vivo radiation dose status in radiotherapy patients using ex vivo and in vivo gene expression signatures. Radiat Res 175:257–265; 2011.

Port M, Seidl C, Ruf CG, Riecke A, Meineke V, Abend M. Reliable and sample saving gene expression analysis approach for diagnostic tool development. Health Phys 103: 159–168; 2012.

Portales-Casamar E, Kirov S, Lim J, Lithwick S, Swanson MI, Ticoll A, Snoddy J, Wasserman WW. Pazar: a framework for collection and dissemination of Cis-regulatory sequence annotation. Genome Biol 8:R207; 2007.

Prise KM, Ahnstrom G, Belli M, Carlsson J, Frankenberg D, Kiefer J, Lobrich M, Michael BD, Nygren J, Simone G, Stenerlow B. A review of DSB induction data for varying quality radiations. Int J Radiat Biol 74:173–184; 1998.

Schultze-Mosgau S, Kopp J, Thorwarth M, Rodel F, Melnychenko I, Grabenbauer GG, Amann K, Wehrhan F. Plasminogen activator inhibitor-i-related regulation of procollagen i (alpha1 and alpha2) by antitransforming growth factor-beta1 treatment during radiation-impaired wound healing. Int J Radiat Oncol Biol Phys 64:280–288; 2006.

Stenerlow B, Karlsson KH, Cooper B, Rydberg B. Measurement of prompt DNA double-strand breaks in mammalian cells without including heat-labile sites: results for cells deficient in nonhomologous end joining. Radiat Res 159:502–510; 2003.

Wang Z, Gerstein M, Snyder M. RNA-seq: a revolutionary tool for transcriptomics. Nat Rev Genet 10:57–63; 2009.

Watt FM, Fujiwara H. Cell-extracellular matrix interactions in normal and diseased skin. Cold Spring Harb Perspect Biol 3:a005124;2011.

Whitehouse CA, Edwards AA, Tawn EJ, Stephan G, Oestreicher U, Moquet JE, Lloyd DC, Roy L, Voisin P, Lindholm C, Barquinero J, Barrios L, Caballin MR, Darroudi F, Fomina J. Translocation yields in peripheral blood lymphocytes from control populations. Int J Radiat Biol 81:139–145; 2005.

Zambon AC, Gaj S, Ho I, Hanspers K, Vranizan K, Evelo CT, Conklin BR, Pico AR, Salomonis N. Go-elite: a flexible solution for pathway and ontology over-representation. Bioinformatics 28:2209–2210; 2012.

Zhou H, Huang S. Mtor signaling in cancer cell motility and tumor metastasis. Crit Rev Eukaryot Gene Expr 20:1–16; 2010.